Thermal characteristics of double-layer thin film target ablated by femtosecond laser pulses*

Gao Xun(高 勋)†, Song Xiao-Wei(宋晓伟), and Lin Jing-Quan(林景全)

School of Science, Changchun University of Science and Technology, Changchun 130022, *China*

(Received 1 August 2010; revised manuscript received 1 September 2010)

Thermal characteristics of tightly-contacted copper–gold double-layer thin film target under ablation of femtosecond laser pulses are investigated by using a two-temperature theoretical model. Numerical simulation shows that electron heat flux varies significantly on the boundary of copper–gold film with different maximal electron temperature of 1.15×10^3 K at 5 ps after ablating laser pulse in gold and copper films, which can reach a balance around 12.6 ps and 8.2 ps for a single and double pulse ablation, respectively, and in the meantime, the lattice temperature difference crossing the gold–copper interface is only about 0.04×10^3 K at the same time scale. It is also found that electron–lattice heat relaxation time increases linearly with laser fluence in both single and double pulse ablation, and a sudden change of the relaxation time appears after the laser energy density exceeds the ablation threshold.

Keywords: femtosecond laser ablation, pulse train, two-temperature model

PACS: 42.65.Re, 44.20.+b, 65.40.De **DOI:** 10.1088/1674-1056/20/2/024210

1. Introduction

Ultrashort pulsed lasers possess exclusive capabilities in limiting the undesirable spread of the thermal process zone during laser ablation process. The interaction of these laser pulses with metals has been intensively studied in the past two decades. In particular, a lot of attention has been paid to investigations of the femtosecond laser ablation of metals.[1−7] Anisimov *et al.* put forward a two-temperature model of metal ablation by ultra-short laser pulse[8] and this model has been widely used for the ultra-short laser processing of metals. Jiang and Tsai investigated dependence of Cu target ablation rate on number of double-pulse under a fixed laser energy density.[9] Dai studied heat propagation characteristic of double-layer metal film with finite difference time domain (FDTD).[10,11] Han *et al.* observed "window time-domain effect" existing between ablation and pulse separation while ablating Cr film with femtosecond double-pulse train.[12]

Multilayer thin films are important components in many microelectronic devices. Thus the transportation of thermal energy through thin films is of vital importance in micro-technological applications. Exploration of temperature-dependent thermal properties is necessary to advance our fundamental understanding of ultrafast heat transportation. However, to our knowledge, there are few reports on ablation of double-layer metal film by use of double laser pulses. In this paper, we study the temperature-dependent thermal properties in a double-layer metal thin film ablated by femtosecond pulsed lasers with the two-temperature model. Effects of the laser pulse number (single or double pulses) on electron heat flux spatial distribution are analysed. Electron–lattice heat relaxation times, spatial distribution fluctuation of electron and lattice temperatures around the boundary of double-layer film are discussed.

2. Theoretical model

When the laser radiation does not induce the interband transitions, the laser heating of metals can be understood as follows. The laser energy is first absorbed by electrons owing to the inverse bremsstrahlung and free electron was heated to larger kinetic energy during several femtosecond. It is followed by a fast energy relaxation within the electron subsystem, thermal diffusion, and an energy transfer to the lattice owing to the electron–phonon coupling. Therefore the spatial and the temporal evolution of the electron and the lattice temperatures (T_e and T_l respectively) can be described by one-dimensional two-temperature diffusion mode.[13] Consider that a metal thin film consists of copper and gold layers ex-

*Project supported by the National Natural Science Foundation of China (Grant No. 60978014), the Natural Science Foundation of Jilin Province (Grant No. 20090523) and the Educational Commission of Jilin Province (Grant No. [2008]297).

†Corresponding author. E-mail: lasercust@yahoo.com.cn

© 2011 Chinese Physical Society and IOP Publishing Ltd

posed to ultrashort pulsed laser from copper layer side, as shown in Fig. 1.

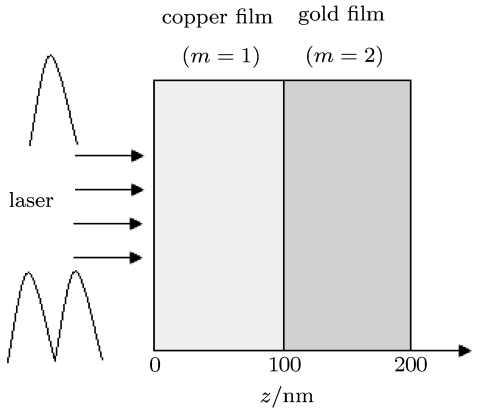


Fig. 1. Femtosecond laser pulses ablated model of double-layer thin films.

The two-temperature heat transport equations in this double-layer metal thin film can be expressed as follows:[14,15]

$$C_{\rm e}^{(m)}\frac{\partial T_{\rm e}^{(m)}}{\partial t} = \nabla(K_{\rm e}^{(m)}\nabla T_{\rm e}^{(m)}) - g(T_{\rm e}^{(m)} - T_{\rm l}^{(m)}) + S^{(m)}(z,t), \quad (1)$$

$$C_{\rm l}^{(m)}\frac{\partial T_{\rm l}^{(m)}}{\partial t} = \nabla(K_{\rm l}^{(m)}\nabla T_{\rm l}^{(m)}) + g(T_{\rm e}^{(m)} - T_{\rm l}^{(m)}), \quad (2)$$

$$S^{(m)}(z,t) = 0.94J\frac{(1-R^{(m)})}{t_{\rm p}\delta^{(m)}}\sum_{n=1}^{n}\exp\left[-\frac{z}{\delta^{(m)}} - 2.77\left(\frac{t-2t_{\rm p}-(n-1)\tau}{t_{\rm p}}\right)^2\right], \quad (3)$$

$$Q_{\rm e}^{(m)}(z) = -K_{\rm e}^{(m)}\partial T_{\rm e}^{(m)}/\partial z, \quad (4)$$

where m indicates a specified metal layer, n is pulse number, τ is the pulse separation time in double pulse laser train. The $C_{\rm e}^{(m)}$ and $C_{\rm l}^{(m)}$ are the electronic heat capacity and the lattice heat capacity respectively, g is a parameter of the transfer of energy between the electrons and the lattice and S is the laser heating source. The z axis is normal to the ablated target surface plane. The $R^{(m)}$ and $\delta^{(m)}$ are the surface reflectivity and optical penetration depth respectively, J is the laser fluence, $t_{\rm p}$ is the laser pulse width, $Q_{\rm e}^{(m)}(z)$ is the heat flux of electron, $k_{\rm e}^{(m)}$ and $k_{\rm l}^{(m)}$ are the electron thermal conductivity and lattice thermal conductivity respectively, which are dependent on thermal properties,[16]

$$k_{\rm e}^{(m)} = \chi^{(m)}\frac{(\mu_{\rm e}^2+0.16)^{5/4}(\mu_{\rm e}^2+0.44)\mu_{\rm e}^2}{(\mu_{\rm e}^2+0.092)^{1/2}(\mu_{\rm e}^2+\eta^{(m)}\mu_{\rm l})}, \quad (5)$$

where $\mu_{\rm e} = T_{\rm e}^{(m)}/T_{\rm F}^{(m)}$, $\mu_{\rm l} = T_{\rm l}^{(m)}/T_{\rm F}^{(m)}$, $T_{\rm F}^{(m)}$ is Femi temperature, $\chi^{(m)}$ and $\eta^{(m)}$ are specific constants of materials, all material constants can be seen in Refs. [16] and [17].

We assume that the interface is perfectly thermal contact and interfacial conditions are assumed to be at $z = 100$ nm, so that

$$Q_{\rm e}^{(1)} = Q_{\rm e}^{(2)}, \quad T_{\rm e}^{(1)} = T_{\rm e}^{(2)}$$
$$Q_{\rm l}^{(1)} = Q_{\rm l}^{(2)}, \quad T_{\rm l}^{(1)} = T_{\rm l}^{(2)}. \quad (6)$$

The initial conditions are assumed for the simulation to be

$$T_{\rm e}^{(n)}(z,0) = T_{\rm l}^{(n)}(z,0) = T_0 = 300\ {\rm K},$$
$$Q_{\rm e}^{(n)}(z,0) = Q_{\rm l}^{(n)}(z,0) = 0. \quad (7)$$

In the process of numerical simulation, the reflectivity of gold film to laser is considered to be zero on the boundary of copper and gold films as copper film thickness is far larger than the optical penetration depth, where there only exists heat transportation as copper–gold film is tightly thermal contact. In addition, calculations of thermal parameters of metals are from Refs. [18] and [19].

3. Results and discussion

3.1. Electron heat flux

The spatial and temporal evolution of the electron heat flux in copper–gold film irradiated by a single or double pulse was simulated with laser energy density of 0.1 J/cm^2 with a laser of 100 fs and 800 nm. The positive heat flux indicates that the heat transition direction is along the laser propagation, the negative value indicates the reverse process. After femtosecond laser pulse irradiation, as shown in Fig. 2, it is interesting to note that the change of electron heat flux around interface of the double-layer film is different from other positions for single and double laser pulse, the electron heat flux rises sharply within the pulse duration outside the region from 98 nm to 102 nm, but drops sharply at 102 nm near the interface. As shown in Fig. 2(a), the electron heat flux at 98 nm rises slowly below 2.5 ps, and then drops to a heat balance between two films at 12.6 ps with a zero electron heat flux. At the position of 102 nm, electron heat flux drops sharply during the laser irradiation and then drops slowly within 1 ps, this is because the electron heat transmission and electron heat flux slowly rise to heat balance, the time is longer than 1 ps. When double pulses with a separation time of 1 ps irradiate

the target, as shown in Fig. 2(b), the electron heat flux around the boundary of double-layer film reaches a heat balance at 8.2 ps. Under the pulse laser train ablation, because the second pulse reheating is compared to the case of single laser pulse, the heat flux shows two peaks/valleys. This result shows that, with fixed ablation laser energy, the arrival time (12.6 ps) of heat balance on the border of the double-layer for single pulse ablation is much longer than that of double pulses (8 ps). With fixed total pulse energy, the time of electron heat flux around the boundary coming to zero for single pulse is longer than that of double pulse. This is due to one single pulse in the double pulse train is with much lower pulse energy in comparison with single pulse case. The electron heat flux is positive at position of 110 nm for both single and double pulse cases, and this is normal heat behaviour while electron transport in the Au film.

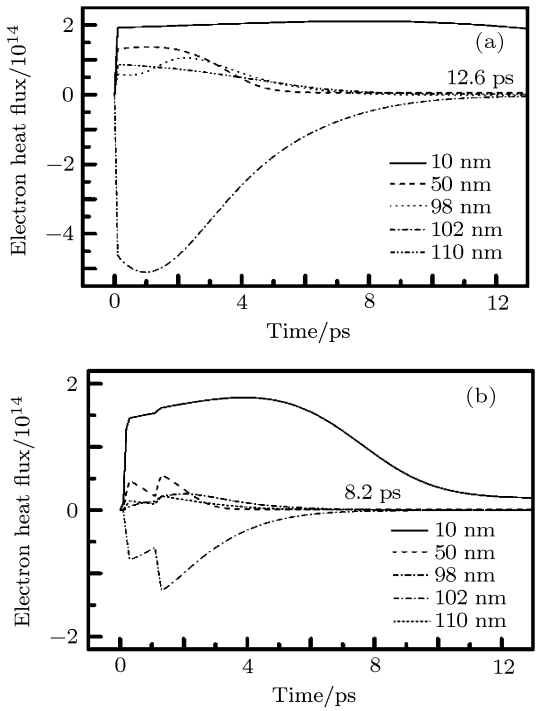


Fig. 2. Electron heat flux evolution at different distances from surface, total laser fluence is 0.1 J/cm^2. (a) One pulse, (b) pulse train (two pulses with separation time of 1 ps).

Figures 3 and 4 show the spatial evolution of electron and lattice temperatures by a pulse train ablation with two pulses separated by 1 ps and the single pulse energy of 0.05, 0.2, 0.5 J/cm^2, and at the time of 0.1 ps and 5 ps after laser pulse interaction. Insets of Fig. 3 are the zoom-in electron temperature distributions around the layer boundary. From Fig. 3, one can see that the maximum temperature difference at 5 ps after laser ablation is 1.25×10^3 K at the position of 2 nm from the layer boundary. It is noted that a dip appears in the electron temperature around 2 nm ahead of film interface and a peak appears behind, and these phenomena become much more obvious at 1 ps and 5 ps after pulse ablation of the target.

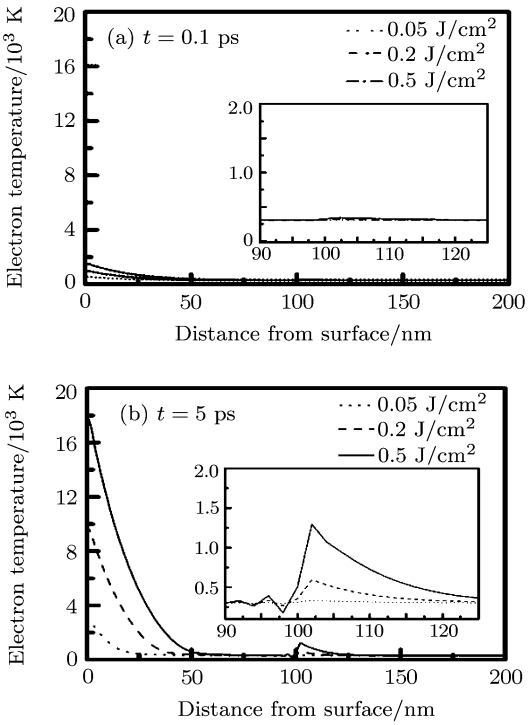


Fig. 3. Electron temperature spatial distribution at different laser fluences of 0.05, 0.2, 0.5 J/cm^2, inset is the electron temperature distribution around the interface.

Furthermore, it is obvious that the increase of electron temperature in the gold side is much larger than the drop of the electron temperature in the copper side since, by regarding the gold film, the copper film works as a heating source and the heat transfers into the gold film from it. The difference of the temperature variations in the gold and copper sides is a result from their different heat capacities. Double dips appear in the spatial distribution of electron temperature around the border at 5 ps after the ablation of laser, in which the first dip is much shallower than the second ones. This is associated with heating of gold film from the copper side by the double laser pulses of 1-ps separation. The second dip is much deeper than the first one, which might be due to the accumulation of heating. The electron heat diffusion follows Fourier's law, and the temperature fluctuation arisen at the border from accumulation of heating can be neglected after 50 ps from the laser pulse ablation, because 50 ps is much longer than the electron–lattice relaxation time and pulse separation leads to the double pulses functioned as a big pulse. It is found that the electron

temperature reaches a peak around 3 nm behind interface of two films, and then drops. This can be used to explain that the electron heat flux within a range of 100 nm to 103.5 nm is negative and becomes positive beyond this range as shown in Fig. 2.

Regarding the spatial and temporal distribution of the lattice temperature, shown in Fig. 4, we find that the maximal temperature difference crossing the border is 0.05×10^3 K, which is much lower than that of the electron temperature (time is 5 ps). There are no obvious variations at the interface of copper–gold films in the first 0.1 ps after the laser irradiation. Because the laser energy is mainly absorbed by free electrons within a skin layer of copper film, this process takes several tenths femtoseconds, and the electron temperature rises locally in the beginning. However, it takes several picoseconds (depends on the laser pulse energy) for the electron to transfer its energy into the lattice at the position of 100 nm away from the target surface.

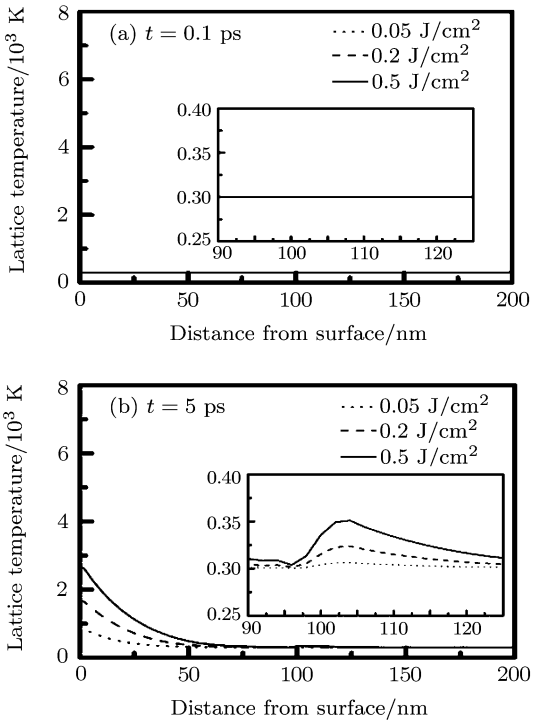


Fig. 4. Lattice temperature spatial distribution at different laser fluences of 0.05, 0.2, 0.5 J/cm^2, inset is the electron temperature distribution around the interface.

Similarly, a small dip of the lattice temperature appears also in the copper side when time is longer than 5 ps, due to its heating action on the gold film, while an increase of the temperature in the gold film is also seen. Spatial distribution of the lattice temperature tends to be balanced and it is affected weakly by the difference of the heat capacities.

3.2. Electron–lattice coupling relaxation time

Electron–lattice heat relaxation time is a dominating parameter for explaining laser–metal interaction. The ablation is called "heat ablation" when the laser pulse duration used is longer than the electron–lattice heat relaxation time of metal, and otherwise the ablation is named as "cold ablation". Dependence of the electron–lattice relaxation time at the target surface on the laser energy density under the cases of single pulse and double pulse ablations is shown in Fig. 5. These simulation results show that the electron–lattice relaxation time in the case of double pulse is much longer than that in the case of single pulse case. A much longer relaxation time under the double pulse ablation is due to that second pulse sees a heated ablation region caused by the first pulse, and heat transportation process between electron and lattice is re-established under the interaction of the second laser pulse which results in an extended electron–lattice relaxation time over a single pulse. Simulation results also show that electron–lattice heat relaxation time increases with laser energy density.

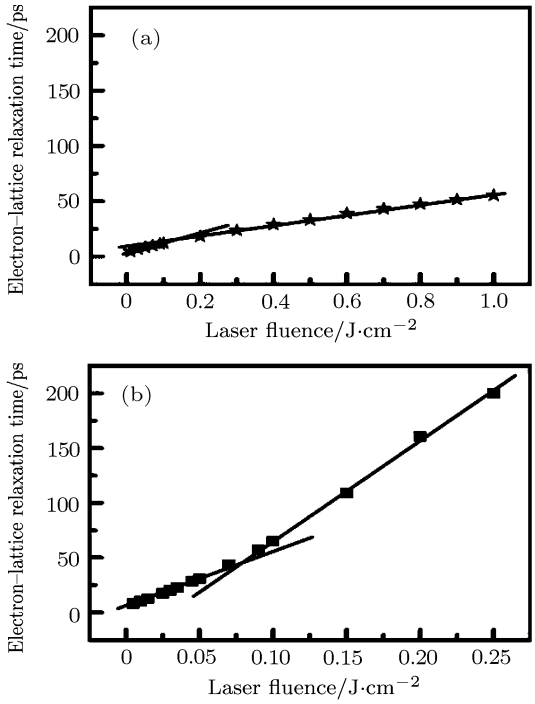


Fig. 5. Electron–lattice relaxation time of double-layer films variation with laser fluence. (a) Single pulse, (b) pulse train (pulse separation time 1 ps).

There are sudden changes in the curves showing dependence of the electron–lattice relaxation time on the laser pulse energy density for both single and double pulse cases. The sudden changes in the curve correspond to laser ablation threshold, which gives a value of 0.14 and 0.128 J/cm^2 for a single and double

pulse cases, respectively. It shows that the ablation threshold is much lower in the double pulse case. The reason is that there is a solid–liquid phase transition on the metal surface[20,21] and vapourization plays a dominating role while topography changes, causing a variation of reflectivity and absorption, heat capacity and heat conductivity,[4,22] all of these parameters have large influence on the electron–lattice heat relaxation.

4. Conclusions

Heat transportation behaviour of femtosecond laser ablation of double-layer metal target is simulated by using FDTD based on two-temperature model. Electron heat flux on the boundary of two films varies significantly under both single and double pulse irradiations with fixed laser fluence of 0.1 J/cm^2, and it takes longer time for the electron flux to reach zero in the case of single pulse than that of double pulse cases. Lattice temperature variation around the film border shows much smaller value in comparison with that of the electron temperature. It is found that electron–lattice relaxation time increases with laser energy density linearly. There exists a sudden change after the laser energy density is higher than the material ablation threshold.

References

[1] Vorobyev A Y, Makin V S and Guo C L 2009 *Phys. Rev. Lett.* **102** 234301

[2] Yamashita Y, Yokomine T, Ebara S and Shimizu A 2006 *Int. J. Thermophys.* **27** 627

[3] Nedialkov N N, Imamova S E and Atanasov P A 2004 *J. Phys.* D: *Appl. Phys.* **37** 638

[4] Vorobyev A Y and Guo C L 2005 *Phys. Rev.* B **72** 195422

[5] Kim J and Na S 2007 *Opt. & Laser Technol.* **39** 1443

[6] Liu Y Q, Zhang J and Liang W X 2005 *Chin. Phys.* **14** 1671

[7] Zhang H Y and Wu S G 2007 *Acta Phys. Sin.* **56** 5314 (in Chinese)

[8] Anisimov S I, Kapeliovich B L and Sov T L 1974 *Phys. JETP* **39** 375

[9] Sim H S, Lee S H and Lee J S 2007 *J. Mech. Sci. Technol.* **21** 1847

[10] Wang H J, Dai W Z and Melnik R 2006 *Int. J. Thermal Sci.* **45** 1179

[11] Dai W Z and Niu T C 2008 *Nonlinear Analysis: Hybrid System* **2** 121

[12] Han Z H, Zhou C H, Dai E W and Xie J 2008 *Opt. Commun.* **281** 4723

[13] Yang J J, Liu W W and Zhu X N 2007 *Chin. Phys.* **16** 2003

[14] Qiu T Q and Tien C L 1992 *Int. J. Heat Mass Transfer* **35** 719

[15] Nolte S, Momma C, Jacobs H and Tünnermann A 1997 *J. Opt. Soc. Am.* B **14** 2716

[16] Schäfer C and Urbassek H M 2002 *Phys. Rev.* B **66** 115404

[17] Balasubramni T, Kim S H and Jeong S H 2009 *Appl. Surf. Sci.* **255** 9601

[18] Christensen B H, Vestentoft K and Balling P 2007 *Appl. Surf. Sci.* **253** 6347

[19] Gray D E 1972 *American Institute of Physics Handbook* 3rd edn. (New York: McGraw-Hill)

[20] Jensen M J, Hasegawa T, Bollinger J J and Dubin D H E 2005 *Phys. Rev. Lett.* **94** 025001

[21] Povarnitsyn M E, Khishchenko K V and Levashov P R 2009 *Appl. Surf. Sci.* **255** 5120

[22] Colombier J P, Combis P, Rosenfeld A, Hertel I V, Audouard E and Stoian R 2006 *Phys. Rev.* B **74** 224106